

CONF 890335-257

Submitted to 1989 Particle Accelerator Conference-Accelerator
Science and Technology - Chicago Illinois, March 20-23, 1989
OPERATIONAL STATUS OF THE BROOKHAVEN NATIONAL LABORATORY ACCELERATOR TEST FACILITY*

K. Batchelor, I. Ben-Zvi, T.S. Chou, R.C. Fernow, J. Fischer, J. Gallardo, H.G. Kirk, R.B. Palmer, C. Pellegrini, J. Sheehan,
T. Srinivasan-Rao, S. Ulc, A. Van Steenbergen, M. Woodlee

Brookhaven National Laboratory,
Upton, New York 11973

I. Biglio, N. Kurnit
Los Alamos National Laboratory
P.O. Box 1663
Los Alamos
New Mexico 87545

K.T. McDonald
Department of Physics
Princeton University
Princeton, New Jersey 08544

BNL--41797-Rev.

DE90 001546

01030

Abstract

Design and operation of a 50 MeV Electron Linear Accelerator utilizing a low emittance ($\gamma \epsilon = 5$ to 10 mm-mrad) radio frequency gun operating at an output energy of 5 MeV and a charge of 1 nC is described. Design calculations and early radio frequency measurements and operational experience with the electron gun utilizing a dummy copper cathode in place of the proposed photocathode emitter are given.

Introduction

The Brookhaven Accelerator Test Facility¹ consists of a 50 to 100 MeV electron beam of about 6 psec pulse length which is synchronized with a 100 GW peak power CO₂ laser used to excite an open accelerating structure capable of sustaining accelerating fields of several hundred MeV/m. The system is shown in schematic form in Figure 1 and consists of a 4.7 MeV radio frequency electron gun² with a photocathode, a momentum selection and pulse compression system, and two s-band travelling wave accelerators sections. The gun and accelerating systems are initially being driven by a single 30 MW klystron resulting in an output energy of about 45 to 50 MeV. At a later stage, a second klystron will be added and the output energy will be increased to about 100 MeV.

Electron Gun

The electron gun, which is shown in Figure 2, is similar to that described by Fraser et al.,³ and is made up of a 1 1/2 cell, pi-mode, resonant, disc loaded structure with the cathode at the beginning of the half cell. Power is coupled via a waveguide operating in the conventional TE₀₁₀ mode through slits situated on the outer wall of each cell. By this means only the pi-mode is excited in the electron gun. The RF-gun design parameters are given in Table I. Initially the photocathode will be made of yttrium metal and will be energized with photons from a frequency quadrupled Nd:Yag laser.

Manufacture of the electron gun has been completed and low-level RF-measurements have been carried out with a dummy copper cathode in place. The field has been adjusted to give essentially the same value at the cathode surface as at the center of the large cell. An axial field plot is given in Figure 3. The loaded Q value has been measured by feeding power into the gun cavity via the waveguide and is shown in Figure 4. A matching section upstream of the waveguide input window was used to match the gun to the waveguide and the input match is shown in Figure 5.

The Injection System

The injection system is designed with three principle features in mind: a) convenient access to the photocathode within the RF-

gun; b) magnetic compression of the electron bunch length; and c) momentum selection to allow the RF-gun to run with a thermionic cathode. All of these objectives are satisfied by basing the injection line on a system of magnetic achromatic double bends with a horizontal slit situated between the the two dipoles at the point of maximum dispersion (see Figure 6). The system will allow for a injection momentum selection of 0.1 %.

The initial quadrupole triplet has the function of capturing a rapidly diverging beam (up to $1\sigma = 28$ mrad) and bringing the electron beam to a double waist at the momentum slit. Because of the mirror symmetry, a double waist at the slit ensures a minimizing of the second-order geometric aberrations through the double bend.

The quadrupole triplet following the double bend will provide for the proper matching of the electron beam into the the linac accelerating sections.

A detailed study of the higher-order effects of the magnetic elements in the injection line are reported in another paper at this conference.⁴

Accelerator System

The linac, as shown schematically in Figure 3, consists of two, 2/3 pi-mode, disc loaded, travelling wave sections each 3.05 meters long, excited by a single XK5 klystron capable of delivering about 30 MW of peak power at a frequency of 2856 MHz with a pulse duration of 6 μ sec.

The RF frequency is derived from a 40.8 MHz oscillator which is also used to synchronize the laser systems used for photocathode excitation and experimental timing. A phase locked oscillator operating at the 70th harmonic is used to drive a series of solid state and triode amplifier stages to obtain the 1 KW of drive power for the klystron. Temperature control of the RF-components and a slow-phase servo system is used to lock the RF-accelerating voltage to the laser systems. The RF systems are designed to run at repetition rates up to 6 Hz which limits the thermal gradients in the system. Power is fed from the klystron through a vacuum waveguide system using high power hybrid junctions and phase shifters to set the correct RF-phase and amplitude for acceleration. Power measurements are made with directional couplers and pumping is achieved via ion pumps connected to waveguide vacuum ports. The accelerating sections and waveguide components were purchased from the Institute for High Energy Physics in Beijing, China and the klystron system was obtained from Stanford Linear Accelerator Center. The water cooling for the accelerating sections and electron gun is temperature controlled to $45 \pm 0.02^\circ$ C. Power to the electron gun is fed through a high power phase attenuator and phase shifter so that the power level and phase can be varied in a continuous way from a few KW up to a maximum of about 12 MW which is well above the design level of 4.5 MW.

*Work performed under the auspices of the U.S. Department of Energy

MASTER

Beam Diagnostics

The ATF beam diagnostics will incorporate non-destructive beam position monitors of the strip line type, Faraday cups for current measurements, and destructive beam profile and position monitors based on a phosphorous screen and CCD camera system. The image is viewed by the camera through an optical system consisting of a 45 degree aluminum mirror, vacuum window and two large aperture commercial lenses. The design includes a means for remotely retracting the screen/mirror sub-assembly, which is in high vacuum, out of the beam and then accurately repositioning it.

Momentum analysis will be done using a bending magnet. The beam profile measurement in the time domain will be done by incorporating an RF-deflection cavity into the beamline. These measurements, momentum and time, will be done by switching off the second dipole of the double bend and analysing the beam profile using the phosphorous screen and CCD camera technique. Furthermore, we plan to use the same setup for emittance measurement using the pepper-pot technique. Since we expect a small beam emittance, we anticipate the need for improved beam emittance diagnostics. We are studying two alternative techniques. One is based on a silicon integrated strip line device which is currently under development. The beam profile will be acquired by sampling the beam with a spatial resolution below 2 microns. Two such devices will yield the beam emittance. The other technique, which we are considering for the beam at the linac output is optical transition radiation from sub-micron thick aluminum foils. To combine both angular divergence and spatial profile we shall use two foils, a mirror quality foil for divergence and a matte foil for profile measurements.

Beam Dynamics

The dynamics of the electron beam coming off the photocathode has been modeled with the programs PARMELA and MASK. General agreement as to the expected characteristics of the electron beam at the RF-gun exit has been obtained using the two programs. Results of the modeling using PARMELA have been previously published.²

The linac beam dynamics was calculated using a modified version of Roger Miller's program LINAC. The input beam was generated using TRANSPORT calculations of the injection system. We have verified that with proper matching of the transverse beam no increase of the transverse normalized emittance occurs at the linac. The longitudinal emittance also does not grow, so that the fractional energy spread decreases by about an order of magnitude. A plot of transverse trajectories along the linac is given in Figure 5.

Controls

The control system for the ATF is based around a MicroVax II color workstation. The data acquisition and control functions use CAMAC electronics in a serial highway configuration. The control system software is built around a graphical interface and database provided by Los Alamos National Laboratory and a CAMAC driver from Kinetic Systems Corporation. At present only the modulator has been incorporated into the control system.

Acknowledgements

We wish to thank our technical staff of H. Ackerman, C. Biscardi, M. Carroll and L. DeSanto for their dedicated efforts in fabricating and assembling all of the electrical and mechanical system and for assisting in the measurements.

References

- [1] K. Batchelor, T.S. Chou, R.C. Fernow, J. Fischer, J. Gallardo, H.G. Kirk, R. Koul, R.B. Palmer, C. Pellegrini, J. Sheehan, T. Srinivasan-Rao, S. Uic, M. Woodie, I. Bigio, N. Kurnit and K.T. McDonald, "The Brookhaven Accelerator Test Facility", Proceedings of the Linear Accelerator Conference, Williamsburg, Virginia (1988)

- [2] K. Batchelor, H. Kirk, J. Sheehan, M. Woodie and K. McDonald, "Development of a High Brightness Electron Gun for the Accelerator Test Facility at Brookhaven National Laboratory." Proceedings of the European Particle Accelerator Conference, Rome, Italy, June 7-11, (1988).
- [3] Fraser et. al., "Photocathodes in Accelerator Application", Particle Proceedings of the 1987, IEEE Particle Accelerator Conference, Washington, DC, pp 1705-1709, March 16-19, 1987.
- [4] X.J. Wang, H.G. Kirk, C. Pellegrini, K.T. McDonald, D.P. Russell, "The Brookhaven Accelerator Test Facility Injection System." Contribution to this conference.
- [5] D.P. Russell, K.T. McDonald, and B. Miller, "A Beam-Profile Monitor for the BNL Accelerator Test Facility (ATF)." Contribution to this conference.
- [6] Xavier Maruyama, Naval Postgraduate School, Monterey, Private communication.

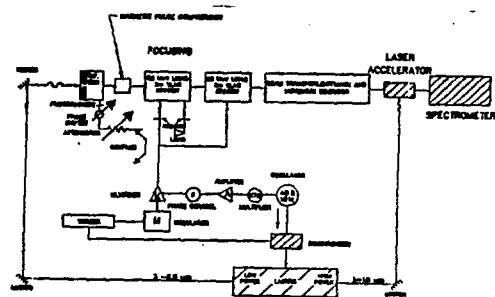


Fig. 1 Schematic of the Accelerator Test Facility.

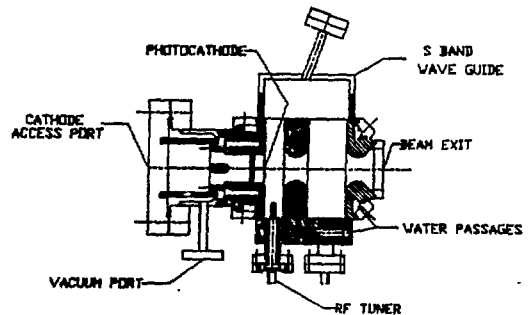


Fig. 2 Schematic of the Electron Gun.

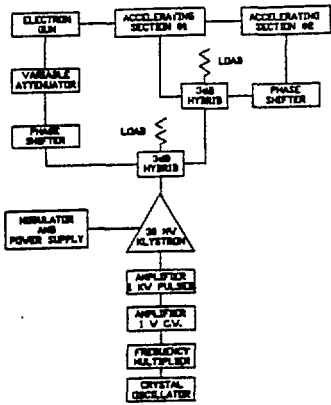


FIGURE 5. RF POWER SYSTEM LAYOUT WITH ONE KLYSTRON

Fig. 3 Schematic of the Linac.

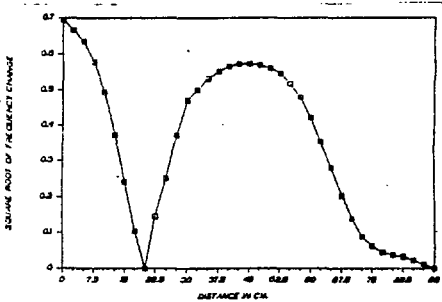


Fig. 4 Axial Electric Field Plot for the Electron Gun.

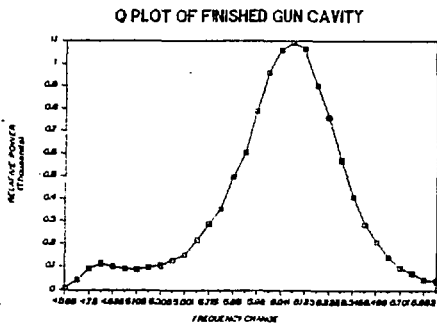


Fig. 5 A plot of the electron gun with power fed in through the waveguide.

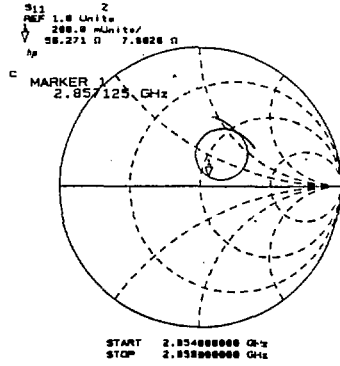


Fig. 6 Input match to the electron gun.

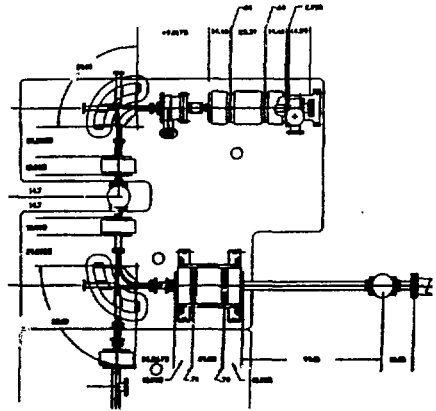


Fig. 7 Schematic of the Injection System.

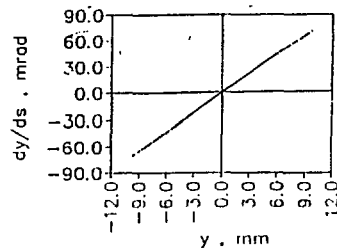


Fig. 8(a) The transverse phase space at the exit of the rf gun for a bunch as given in the table. $\sigma_x = 4.2$ mm, $\sigma_x = 28$ mrad, and $\epsilon_x = 7.3$ mm-mrad.

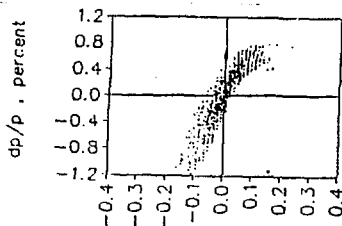


Fig. 8(b) The longitudinal phase space at the exit of the gun. $\sigma_z = 0.6$ mm, and $\sigma_E = 17$ keV.

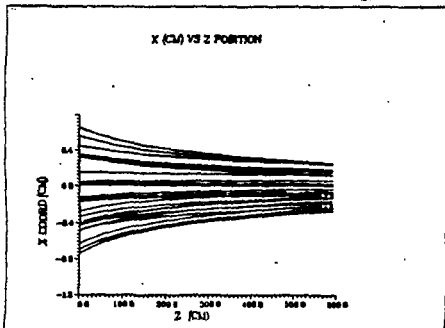


Fig. 9 Ray plot of beam through the accelerating sections.

Table I. RF Gun Design Parameters

Structure type	Resonant
Structure inner diameter, mm	83.08
Structure length, mm	78.75
Number of cells	1+1/2
Operating frequency, GHz	2.856
Beam Energy, MeV	4.85
Beam aperture, mm	20
Shunt Impedance, MΩ/m	57
Cavity Q	11,800
Max. Surface Electric Field, MV/m	118
Average accelerating gradient, MV/m	66.6
Electric field on cathode, MV/m	100
Cavity Stored Energy, J	3.5
Cavity Peak Power, MW	5.3

Emittance Parameters

Laser spot radius (σ in mm)	3
Laser pulse width (σ in psec)	2
Charge in bunch (n Coulomb)	1
ϵ_x^\dagger at cathode (mm-mrad)	3.5
$\Delta\epsilon_x$ due to self fields	6.2
$\Delta\epsilon_x$ due to rf fields	1.4
ϵ_x at exit	7.3
Beam energy spread (σ in keV)	17
Exit bunch length (σ in mm)	0.6
Exit bunch radius (σ in mm)	4.2
Exit beam angular divergence (σ in mrad)	28

$$\dagger \epsilon_x = \frac{1}{mc} \sqrt{\langle x^2 \rangle \langle xp_x^2 \rangle - \langle xp_x \rangle^2} = \sqrt{\langle x^2 \rangle \langle \gamma^2 \beta_x^2 \rangle - \langle x\gamma\beta_x \rangle^2}$$

Table I RF Gun Design Parameters.

DISCLAIMER

This report was prepared as an account of work sponsored by an agency of the United States Government. Neither the United States Government nor any agency thereof, nor any of their employees, makes any warranty, express or implied, or assumes any legal liability or responsibility for the accuracy, completeness, or usefulness of any information, apparatus, product, or process disclosed, or represents that its use would not infringe privately owned rights. Reference herein to any specific commercial product, process, or service by trade name, trademark, manufacturer, or otherwise does not necessarily constitute or imply its endorsement, recommendation, or favoring by the United States Government or any agency thereof. The views and opinions of authors expressed herein do not necessarily state or reflect those of the United States Government or any agency thereof.